Supplementary Information

Cross-linking Zr-based Metal-Organic Polyhedra via Postsynthetic Polymerization

Dongsik Nam[1], Jihyun Huh[1], Jiyoung Lee[1], Ja Hun Kwak[2], Hu Young Jeong[3], Kyungmin Choi[4], and Wonyoung Choe*,[1]

[1]Department of Chemistry, [2]Department of Chemical Engineering, and [3]UNIST Central Research Facilities,

Ulsan National Institute of Science and Technology, 50 UNIST-gil, Ulsan 44919, Republic of Korea.

[4]Department of Chemical and Biological Engineering, Sookmyung Women's University, 100 Cheongpa-ro 47-gil, Seoul 04310, Korea

*Corresponding author choe@unist.ac.kr

Methods

Synthesis of UMOP-1-NH$_2$. To a 5mL vial, Cp$_2$ZrCl$_2$ (17.5 mg, 0.06 mmol), 2-aminoterephthalic acid (5.4 mg, 0.03 mmol), DEF (1mL) and H$_2$O (150 μL) were added. The mixture became clear yellow solution after sonication. The solution was heated in preheated oven at 60°C for 8h followed by 4h cooling. Yellow cubic crystals were synthesized and washed with fresh DEF.

Syntheses of CLMOPs. After removing DEF used for the last wash of UMOP-1-NH$_2$ crystals, a solution of DMA (2 mL) and acyl chloride (suberoyl chloride (8.45 μL, 0.046 mmol) for CLMOP-1*a*, sebacoyl chloride (10 μL, 0.046 mmol) for CLMOP-1*b*, dodecanedioyl dichloride (11.7 μL, 0.046 mmol) for CLMOP-1*c*) was added to the crystals. Then, the sample was gently shaken on a nutator at room temperature for 3 days. Pale yellow crystals were obtained and washed with DMA.

Digestion Method. Digestion is based on a method using CsF[1]. 24 mg of CsF was dissolved in 450 μL of DMSO-d$_6$ and 250 μL of D$_2$O. CsF solution was added to about 3 mg of activated CLMOP sample. Then, the mixture was sonicated for 10 min.

High angle annular dark field (HAADF) scanning transmission electron microscopy. HAADF STEM image was taken by using a JEOL JEM-2100F with a probe-side spherical aberration (Cs) corrector at an acceleration voltage of 200 kV.

Single crystal X-ray diffraction. Single crystal X-ray diffraction (SCXRD) data of UMOP-1-NH$_2$ and CLMOP-1*c* were obtained at the Pohang Accelerator Laboratory (PAL), Korea. The SCXRD data of UMOP-1-NH$_2$ were collected at 2D beamline (2014-3rd-2D-024) at PAL, at 100 K with ADSC Quantum-210 detector at 2D SMC with Mo Kα radiation (λ = 0.70001 Å). The instrument was a Rigaku R-axis Rapid II with Rapid auto software, R-axis series, Rigaku Corporation. For data collection, the ADSC Q210 ADX program[2] was used, and HKL3000[3] for cell refinement. For solving crystal structure, directed method was used and the structure was refined by full-matrix least-squares calculations using the SHELXTL program package[4]. SQUEEZE protocol in PLATON[5] was used to treat disordered solvent and cation.

SCXRD data of CLMOP-1*c* were collected at 6D beamline (2016-2nd-6D-A011) at PAL, with Rayonix Ms225-HS detector at 134K (λ = 0.66000 Å). For data collection, MxDC software was used, and HKL2000[3] for cell refinement. The crystal structure was refined with SHELXTL program package[4]. Disordered solvent, cation, and alkyl chain were treated with PLATON[5].

Crystallographic data have been deposited with Cambridge Crystallographic Data Centre: Deposit number CCDC 1520038 (UMOP-1-NH$_2$) and CCDC 1520037 (CLMOP-1*c*).

Powder X-ray diffraction. PXRD pattern of CLMOP-1c was collected at 2D beamline (2016-2nd-2D-023) at PAL. Powder of CLMOP-1*c* were packed in the 0.3 mm diameter (wall thickness is 0.01 mm) capillary and the diffraction data measured transparency as Debye-Scherrer at 100K with the 120 mm of detector distance in 15 sec exposure with synchrotron radiation (λ = 1.2 Å) on an ADSC Quantum-210 detector at 2D SMC with a silicon (111) double crystal monochromator (DCM). The PAL BL2D-SMDC program[6] was used for data collection, and Fit2D program[7] was used converted 2D to 1D pattern and wavelength and detector distance refinement.

General measurements. Laboratory PXRD data were recorded on a Bruker D2 phaser diffractometer (Cu radiation, λ=1.54184 Å). The tube voltage and current were 30 kV and 10 mA. A step size of 2θ is 0.02°. ^{1}H-NMR data were collected on an Agilent FT-NMR spectrometer (400 MHz). Gas sorption study was performed on a Micromeritics ASAP 2020 instrument. FTIR spectra were recorded on a Varian 670/620 spectrometer equipped with an ATR detector. ESI-MS data were collected on a Synapt G2 at Ochang branch of the Korea Basic Science Institute (KBSI).

Reverse experiment

Instead of cross-linking tetrahedral cages, we tested the reverse experiment whereby synthesized amide dimers were combined with Zr ions to create a new MOFs. We synthesized the amide dimers generated from the crosslinking reaction. With the ligand, MOF synthesis was attempted with the same condition used for synthesis of UMOP-1-NH$_2$. The result was the formation of a gel-like material which might be due to highly flexible alkyl groups preventing hydrogen bonding among tetrahedral cages in solution.

Table S1. Crystallographic data for UMOP-1-NH$_2$.

	UMOP-1-NH$_2$
Molecular formula[a]	$(Zr_{12}C_{108}H_{102}O_{40}N_6)Cl_6((C_2H_5)_2NH_2)_2$
Temperature	100K
Crystal system	Cubic
Space group	*Fm-3m*
a (Å)	36.748(4)
V (Å^3)	49626(17)
Z	8
ρ_{calc} (g·cm^{-3})	0.958
μ (mm^{-1})	0.559
R_1, *I* > *2σ(I)*	0.0758
wR_2, *I* > *2σ(I)*	0.3085

[a]Disordered solvent and cation were treated with the SQUEEZE tool in PLATON[5]. $(C_2H_5)_2NH_2^+$ was included in molecular formula.
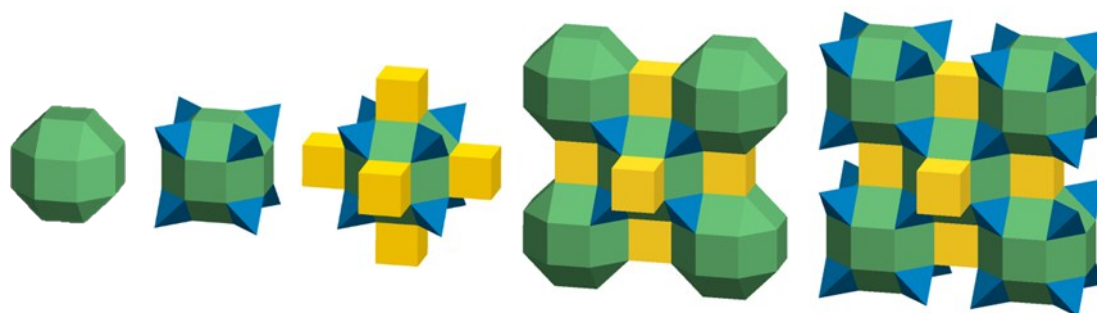
Figure S1. Packing pattern of UMOP-1-NH$_2$. Blue tetrahedrons indicate UMOP-1-NH$_2$ cages. Other pores are described as rhombicuboctahedrons (green) and cubes (yellow). Chloride ions are in yellow cubes with cuboctahedral geometry as shown in Figure S2.
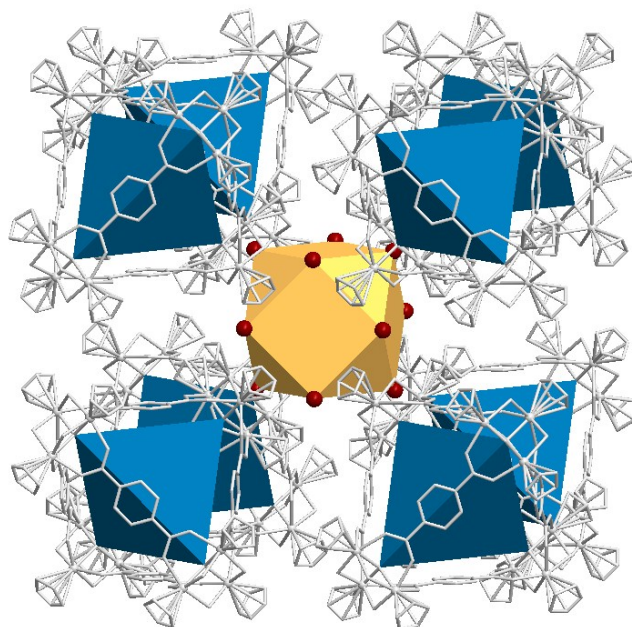

Figure S2. Cl$^-$ ions (dark red balls) interacting with UMOP-1-NH$_2$ cages (blue) through hydrogen bonding. Twelve Cl$^-$ ions form a cuboctahedral shape (yellow), which is in yellow cube in Figure S1. Eight Cl$^-$ ions balance 8+ charge from neighboring eight vertexes of UMOP-1-NH$_2$ cages, having respective 1+ charge. Remaining four Cl$^-$ ions are balanced by four (C$_2$H$_5$)$_2$NH$_2^+$ cations.
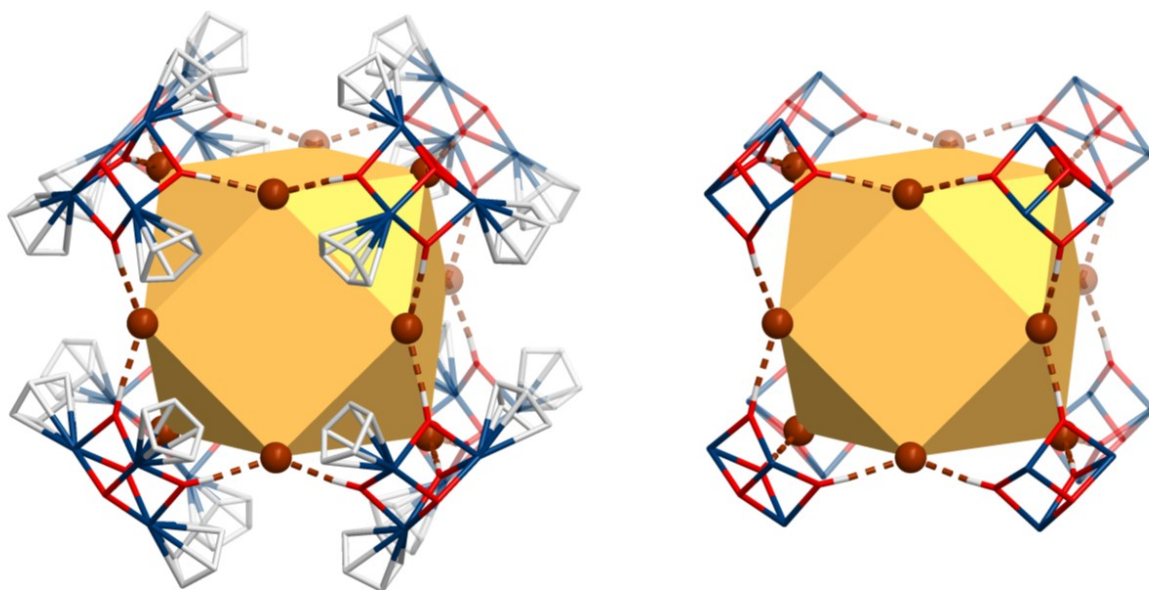
Figure S3. Hydrogen bonding between Zr clusters and Cl⁻ ions (dark red balls). Three μ_2-OH groups in each Zr cluster interact with Cl⁻ ions, resulting in cuboctahedral geometry.

Evidence for existence of $(C_2H_5)_2NH_2^+$ cation

To prove Cl$^-$ ions, shown in Figure S2, are fully occupied, we needed to prove presence of cation for charge balance. Although $(C_2H_5)_2NH_2^+$ cation was not defined in single crystal X-ray diffraction data, we identified the cation in ^{1}H-NMR data of activated UMOP-1-NH$_2$, by comparing with the spectrum of $(C_2H_5)_2NH_2Cl$, purchased from TCI (Figure S3, S4). As shown in Figure S3, peaks of $(C_2H_5)_2NH_2^+$, detected at 3 ppm and 1.3 ppm, are also observed in the spectrum of activated UMOP-1-NH$_2$. The integration ratio of peaks at 3 ppm and 1.3 ppm was 2 : 3 in both spectra of the cation and activated UMOP-1-NH$_2$. By comparing the integration ratio of peaks from Cp ring and the cation, we identified sixteen $(C_2H_5)_2NH_2^+$ cations are incorporated in 1 unit cell of UMOP-1-NH$_2$. The number of cation corresponded to the required positive charge for charge balance of UMOP-1-NH$_2$ framework. Peaks at 7~8 ppm represented protons of BDC-NH$_2$ ligand. Protons of Cp rings were detected at 6.6 ppm.
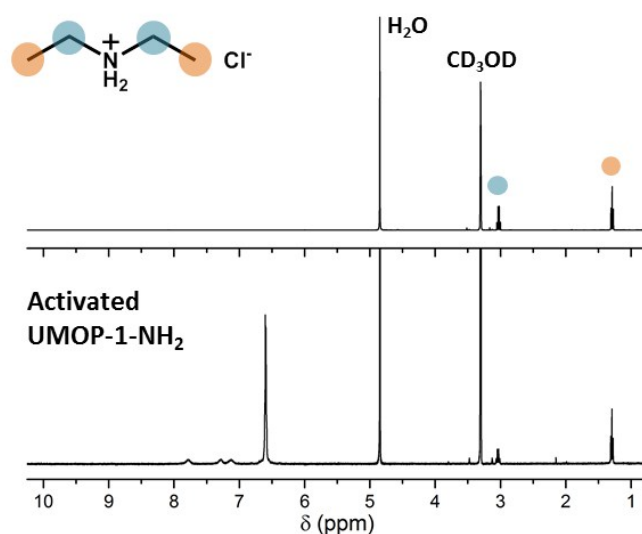
Figure S4. ^{1}H-NMR spectra of $(C_2H_5)_2NH_2Cl$ (top) and activated UMOP-1-NH$_2$ (bottom). Protons of ethyl group in the cation are observed at 3 ppm and 1.3 ppm. Peaks from $(C_2H_5)_2NH_2^+$ are also observed in the spectrum of activated UMOP-1-NH$_2$. Peaks at 7~8 ppm are from BDC-NH$_2$, and a peak at 6.6 ppm is from Cp rings in the spectra of activated UMOP-1-NH$_2$.
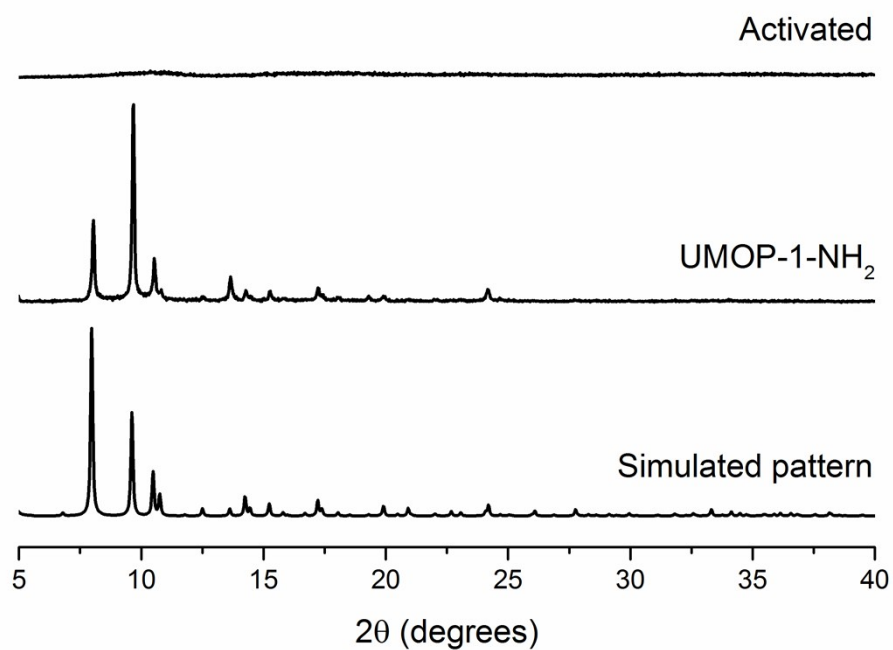
Figure S5. Simulated and experimental powder X-ray diffraction patterns of UMOP-1-NH$_2$. UMOP-1-NH$_2$ sample was ground before measurement to reduce preferred orientation. After activation, UMOP-1-NH$_2$ lost crystallinity.

N₂ adsorption, pore size distribution, and CO₂ adsorption

For gas sorption measurements, 10 times larger scale was used in synthesis of UMOP-1-NH$_2$. The sample was washed with DEF (10 mL $\times$ 4) for 2 days, and with CHCl$_3$ (10 mL $\times$ 4) for 2days. The sample was activated on a sorption instrument at 65°C for 6 hrs.

For isosteric heat of adsorption (Q$_{st}$) calculation, CO$_2$ isotherms at 273K and 293K were fitted with dual-site Langmuir-Freundlich equation (eq 1). With the fitted parameters and Clausius-Clapeyron equation, Q$_{st}$ value was calculated[8].

$$q = \frac{q_{sat,A}b_A p^{\alpha_A}}{1 + b_A p^{\alpha_A}} + \frac{q_{sat,B}b_B p^{\alpha_B}}{1 + b_B p^{\alpha_B}}$$

Eq 1. Dual-site Langmuir-Freundlich equation
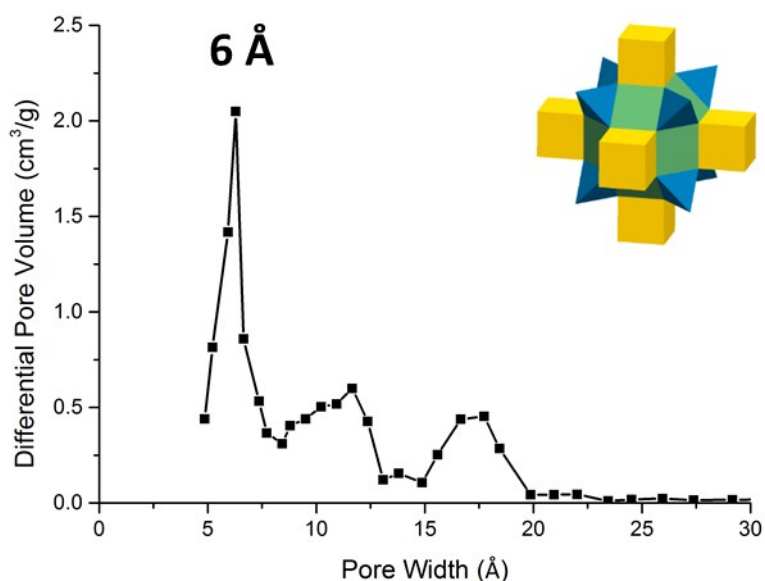
Figure S6. Pore size distribution of UMOP-1-NH$_2$ deduced from N$_2$ isotherms at 77K with the NLDFT model. A sharp peak at 6 Å represents pore size of the tetrahedral cages. Although UMOP-1-NH$_2$ became amorphous after activation, observed pore sizes were similar to theoretical pore sizes of cube (10 Å) and rhombicuboctahedron (18 Å).
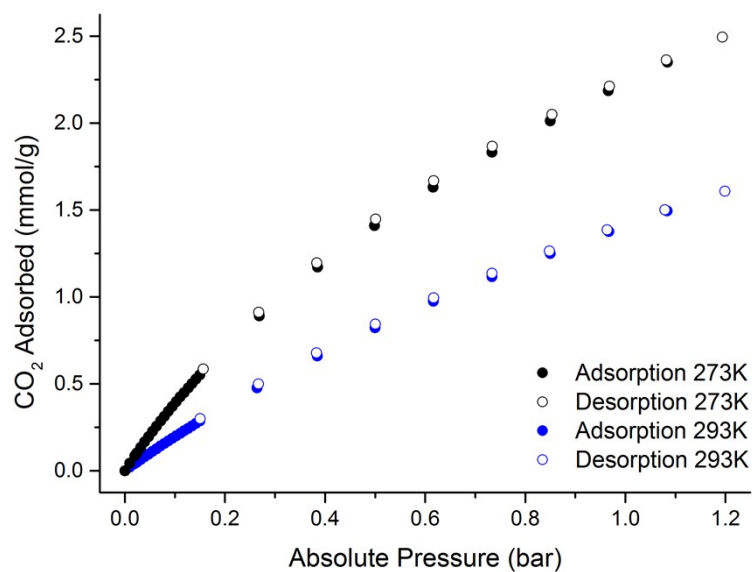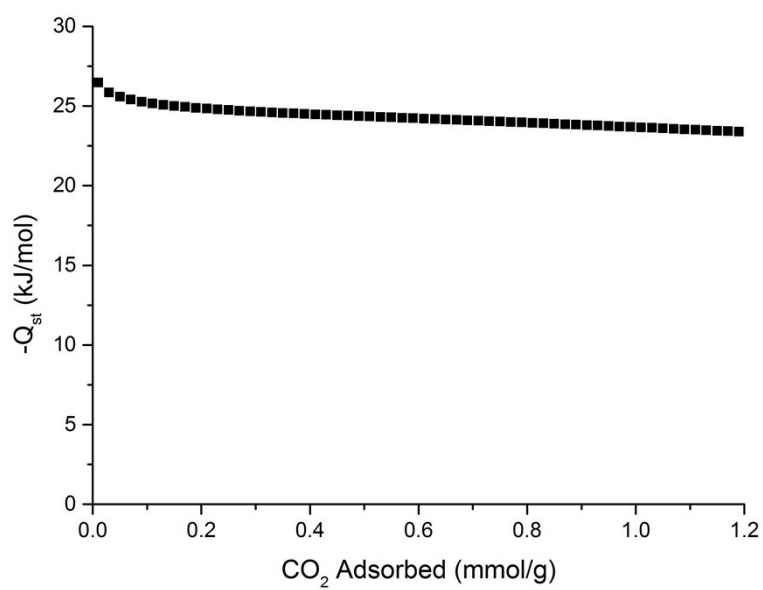
Figure S7. CO_2 isotherms of UMOP-1-NH$_2$ at 273K and 293K.
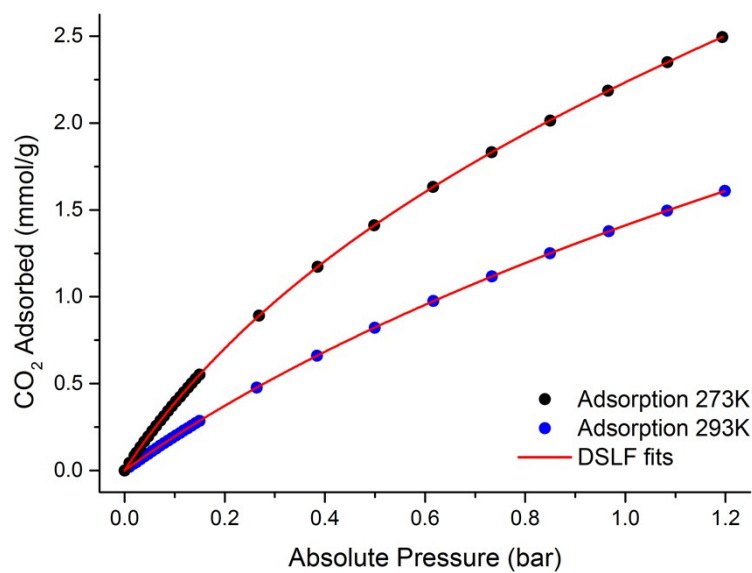
Figure S8. CO_2 isotherms and dual-site Langmuir-Freundlich fits of UMOP-1-NH$_2$ at 273K and 293K.

**Table S2.** Fitted parameters from CO_2 isotherms of UMOP-1-NH$_2$.

	$q_{sat,A}$ (mmol/g)	b_A (bar^{-1})	α_A	$q_{sat,B}$ (mmol/g)	b_B (bar^{-1})	α_B	R^2
CO_2 273K	3.929	1.029	0.976	2.836	0.0927	2.018	0.999999
CO_2 293K	1.45	0.815	0.981	6.958	0.123	1.011	0.999999

Figure S9. Isosteric heats of adsorption (Q_{st}) calculated from CO_2 isotherms of UMOP-1-NH$_2$.

**N$_2$ isotherms & pore size distribution of UMOP-1-NH$_2$ and UiO-66-NH$_2$**

UMOP-1-NH$_2$ and UiO-66 have structurally similar tetrahedral cages. Pore size distribution (PSD) data of the two were deduced from N$_2$ isotherms to identify similar pore size experimentally. The synthesis of UiO-66-NH$_2$ was based on the recipe[9] from Farha and co-workers. As-synthesized UiO-66-NH$_2$ showed PXRD pattern consistent with the simulated pattern of UiO-66 (Figure S12). PSD data of UiO-66-NH$_2$ represented sharp peak at ~6 Å, as observed in the data of UMOP-1-NH$_2$ (Figure S14). N$_2$ isotherms of UiO-66-NH$_2$ revealed the uptake up to ~350 cm^3·g^{-1} (Figure S13) and the BET surface area of 1318 m^2·g^{-1}, suggesting the existence of defects[9].

simulated pattern of UiO-66

as-synthesized UiO-66-NH$_2$

2θ (degrees)
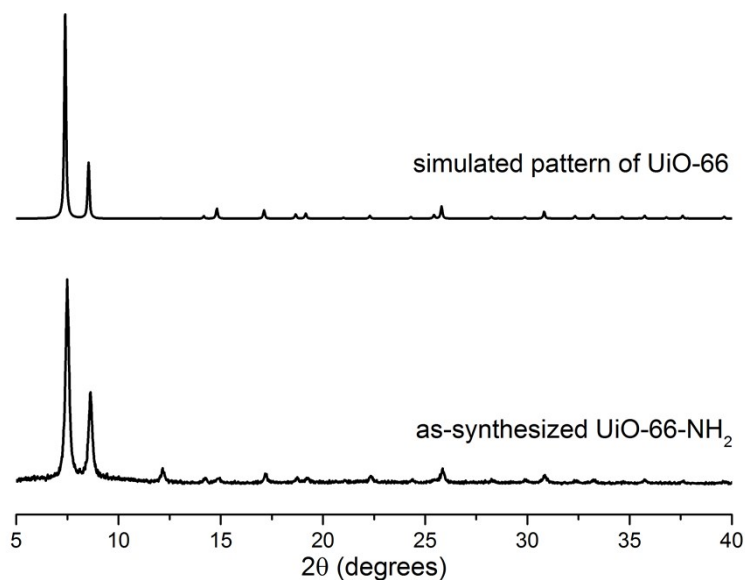
Figure S10. PXRD pattern of simulated UiO-66 and as-synthesized UiO-66-NH$_2$.
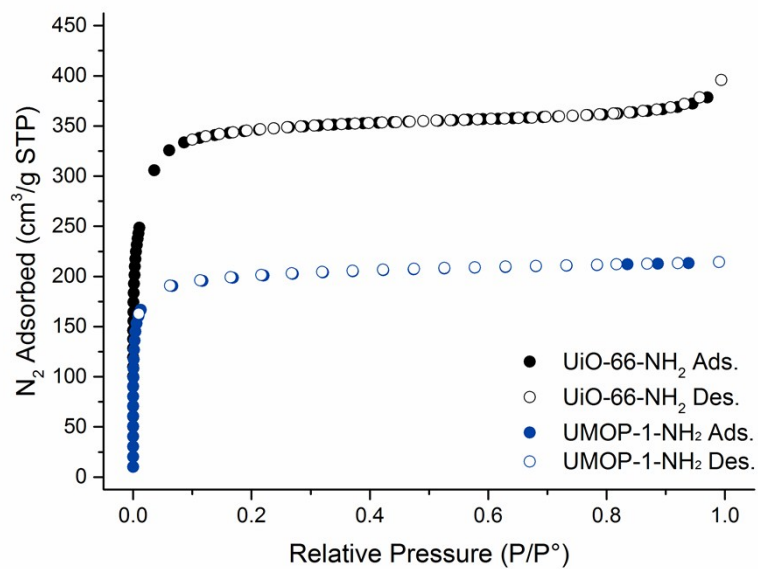
Figure S11. N_2 isotherms of UiO-66-NH$_2$ and UMOP-1-NH$_2$ at 77K. The BET surface area of UiO-66-NH$_2$ is 1318 m^2·g^{-1}, suggesting the presence of defects in the framework[9].
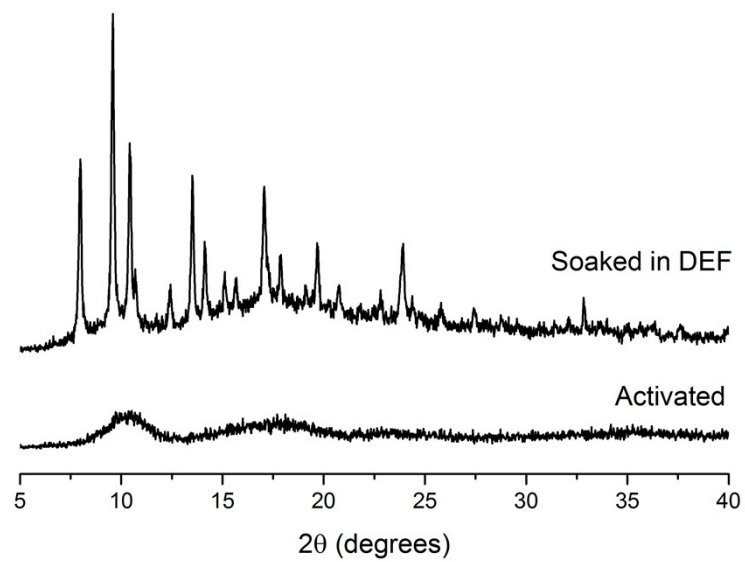
Figure S12. Powder X-ray diffraction pattern of activated UMOP-1-NH$_2$ (bottom). Crystallinity was slightly recovered when the activated UMOP-1-NH$_2$ was soaked in DEF (up).
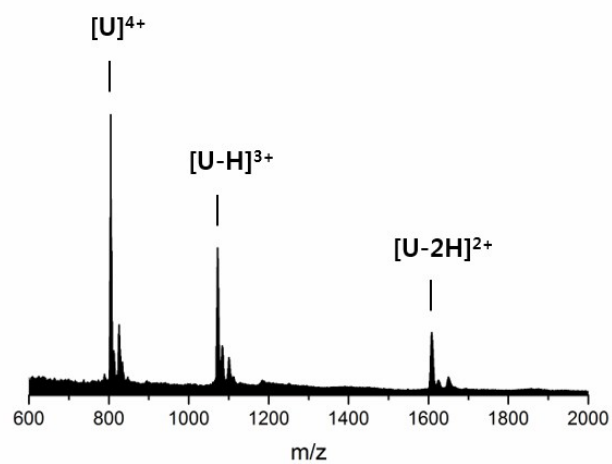
Figure S13. Electrospray ionization mass spectrum of UMOP-1-NH$_2$ solution in MeOH. Mass to charge ratio values of [U]$^{4+}$, [U-H]$^{2+}$, and [U-3H]$^{2+}$ were observed at 804.5, 1072.2, and 1608.0, respectively (U: one UMOP-1-NH$_2$ cage without Cl$^-$ ion). Theoretical values are 804.7, 1072.6, and 1608.3, respectively.

a

b
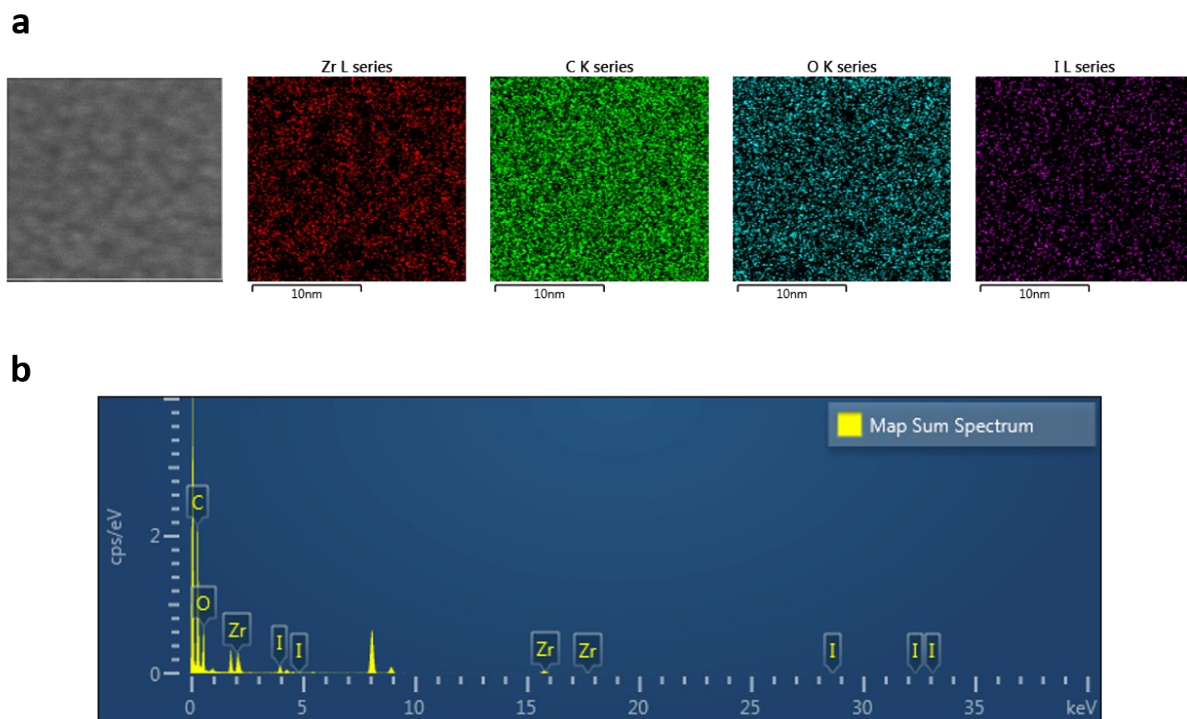
Figure S14. (a) Elemental mapping images and (b) Energy-dispersive X-ray spectrum of UMOP-1-NH$_2$ particles. Existence of Zr element revealed distribution of UMOP-1-NH$_2$ particle. Iodine was added in sample preparation to enhance image quality.
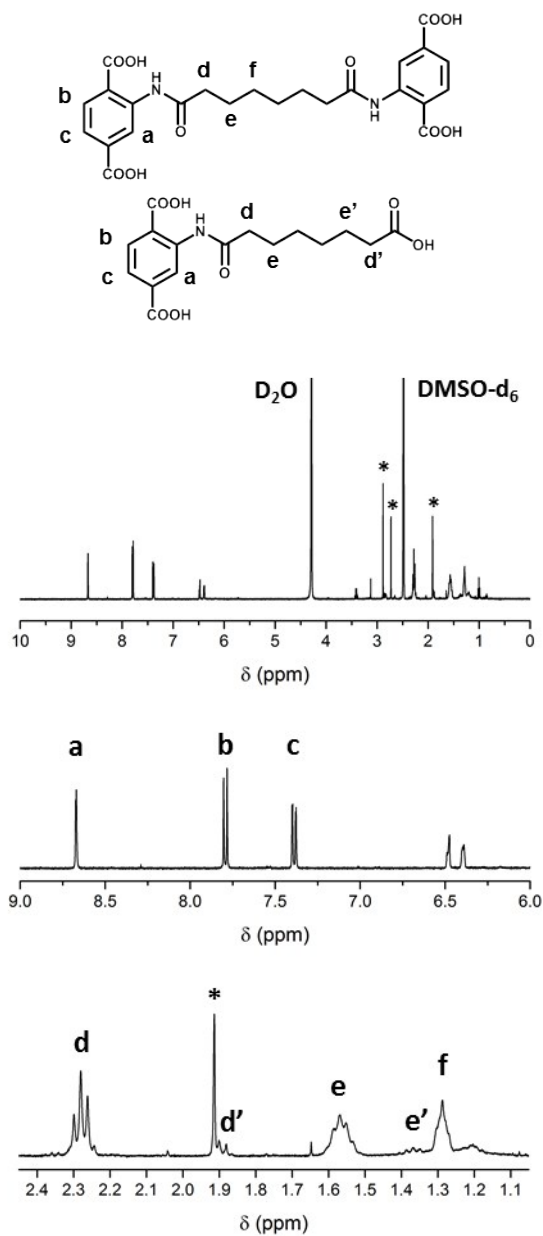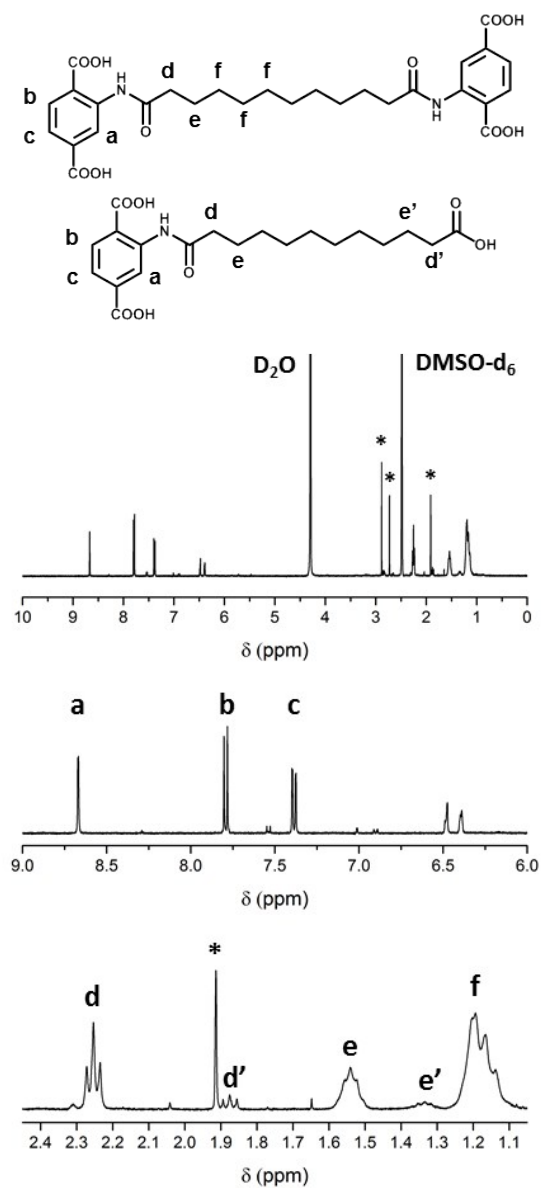
Figure S15. ^{1}H-NMR spectra of CLMOP-1*a* digested with CsF. Because BDC-NH$_2$ ligands are interconnected by suberoyl chloride, amide dimers (top) are formed after digestion. Peaks of a, b, and c correspond to protons of phenyl rings. Peaks of d, e, and f are from alkyl chains. Peaks of d' and e' with relatively small intensity are also observed, suggesting the existence of amide monomer. (*: DMA)
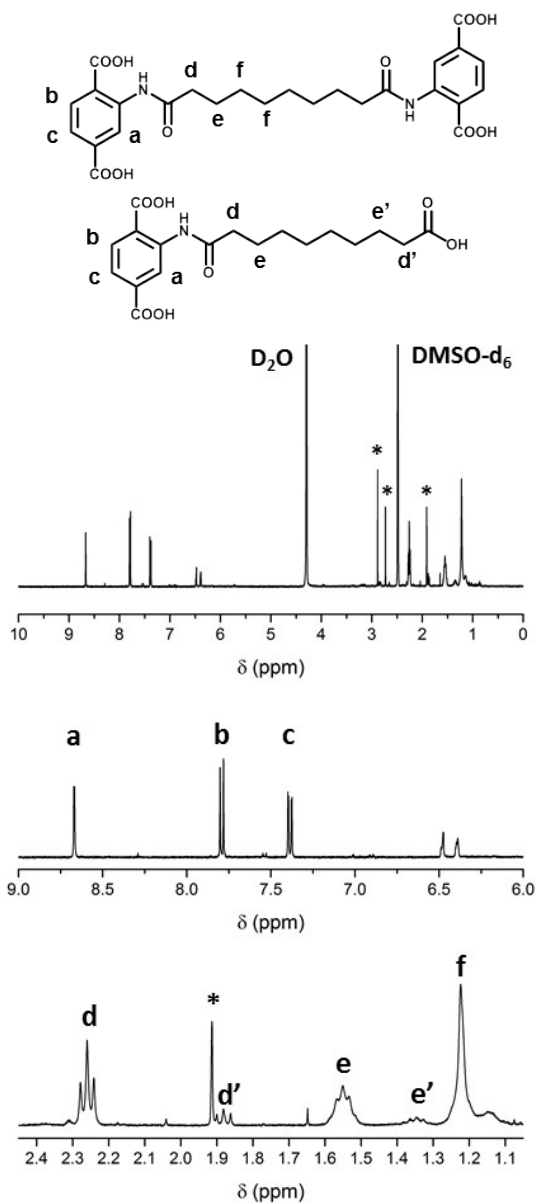
Figure S16. ^{1}H-NMR spectra of CLMOP-1*b* digested with CsF. Because BDC-NH$_2$ ligands are interconnected by sebacoyl chloride, amide dimers (top) are formed after digestion. Peaks of a, b, and c correspond to protons of phenyl rings. Peaks of d, e, and f are from alkyl chains. Peaks of d' and e' with relatively small intensity are also observed, suggesting the existence of amide monomer. (*: DMA)

Figure S17. ^{1}H-NMR spectra of CLMOP-1*c* digested with CsF. Because BDC-NH$_2$ ligands are interconnected by dodecanedioyl dichloride, amide dimers (top) are formed after digestion. Peaks of a, b, and c correspond to protons of phenyl rings. Peaks of d, e, and f are from alkyl chains. Peaks of d' and e' with relatively small intensity are also observed, suggesting the existence of amide monomer. (*: DMA)

Table S3. Proportion of ligand interconnected by acyl chloride linker, calculated from ^{1}H-NMR data

|	Ligand forming amide dimer	Ligand forming amide monomer	BDC-NH$_2$
CLMOP-1*b*	85%	13%	2%
CLMOP-1*c*	88%	9%	3%
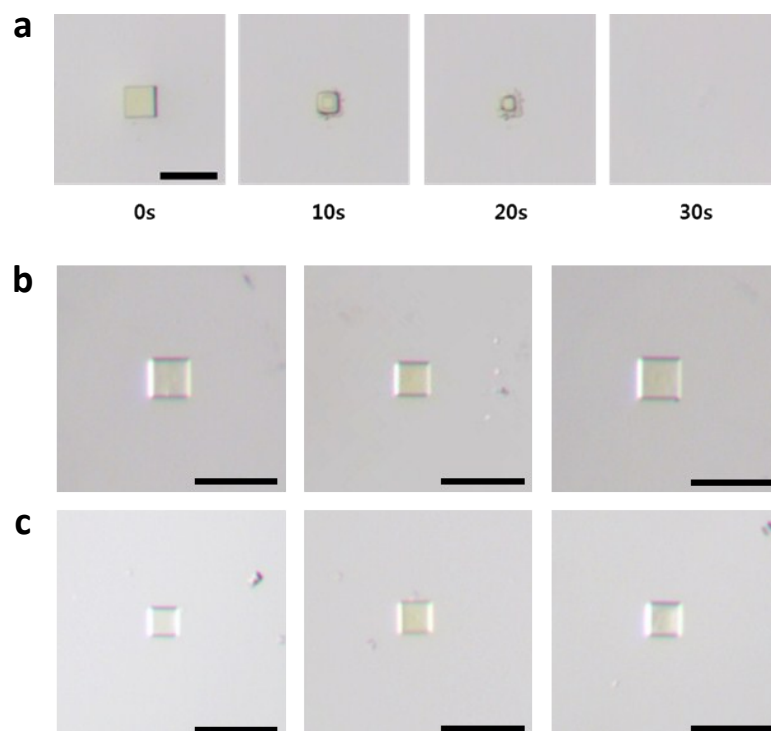
Figure S18. Solubility of UMOP-1-NH$_2$ and CLMOPs in MeOH. (a) Optical microscope images of UMOP-1-NH$_2$ dissolving in MeOH. (b) As-synthesized CLMOPs, and (c) CLMOPs shaken in MeOH for 2 days; from left: CLMOP-1*a*, -1*b*, and -1*c*. Scale bar represents 0.1 mm.
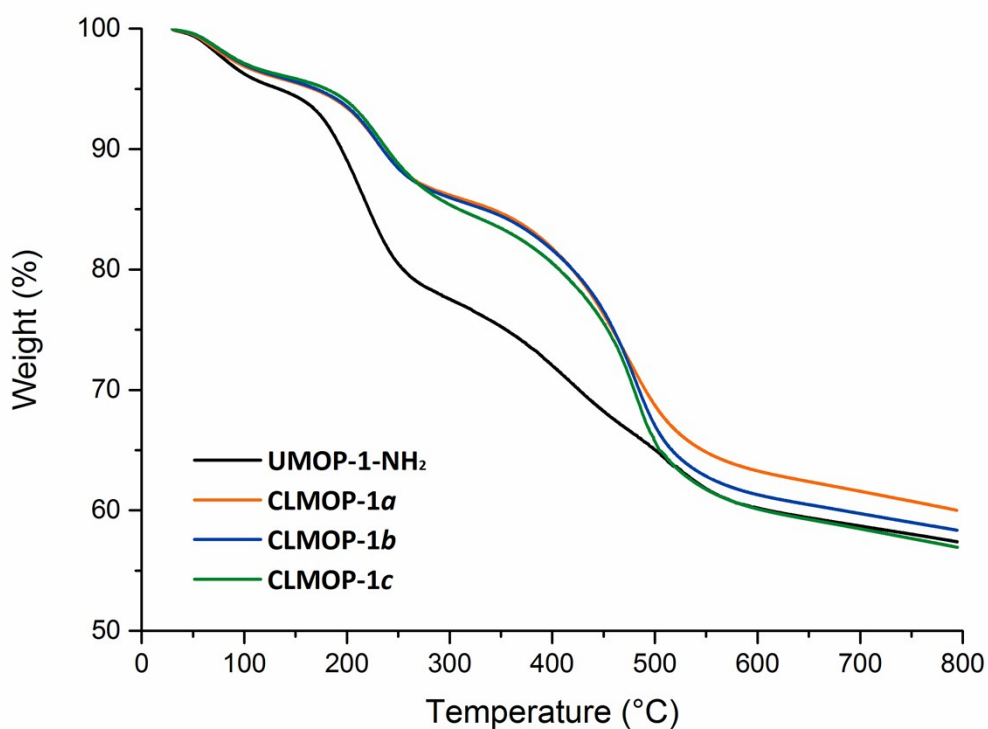
Figure S19. Thermogravimetric analytical traces of activated UMOP-1-NH$_2$ and CLMOPs. Compared to UMOP-1-NH$_2$, CLMOPs show less weight loss at ~200 °C and larger weight loss at ~450 °C. Such difference in weight loss suggests CLMOPs have larger weight of organic moieties. The increased weight is attributed to the incorporation of alkyl chains derived from condensation with acyl chloride linkers.
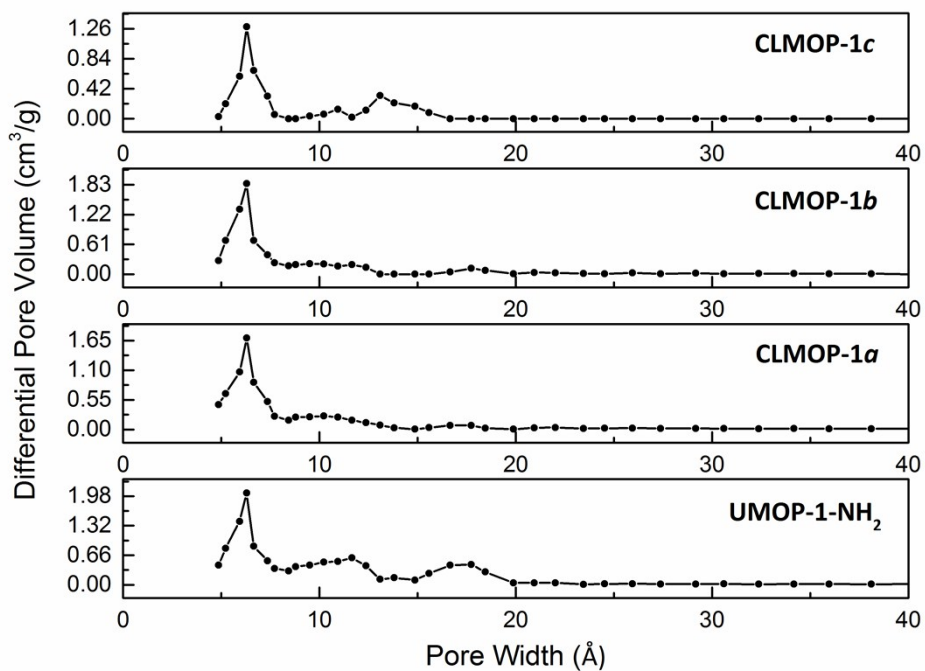
Figure S20. Pore size distribution of UMOP-1-NH$_2$ and CLMOPs. Pore of tetrahedral cage with the width of ~6 Å is observed in both UMOP-1-NH$_2$ and CLMOPs.
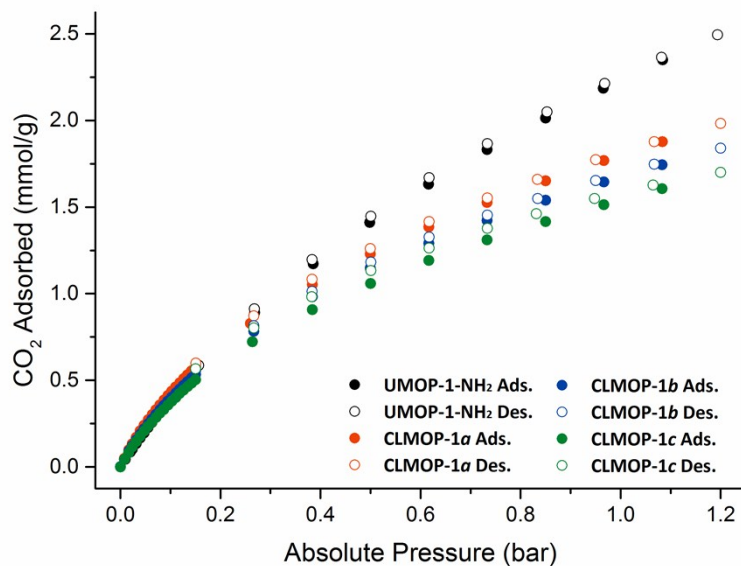
Figure S21. CO$_2$ isotherms (273K) of UMOP-1-NH$_2$ and CLMOPs.
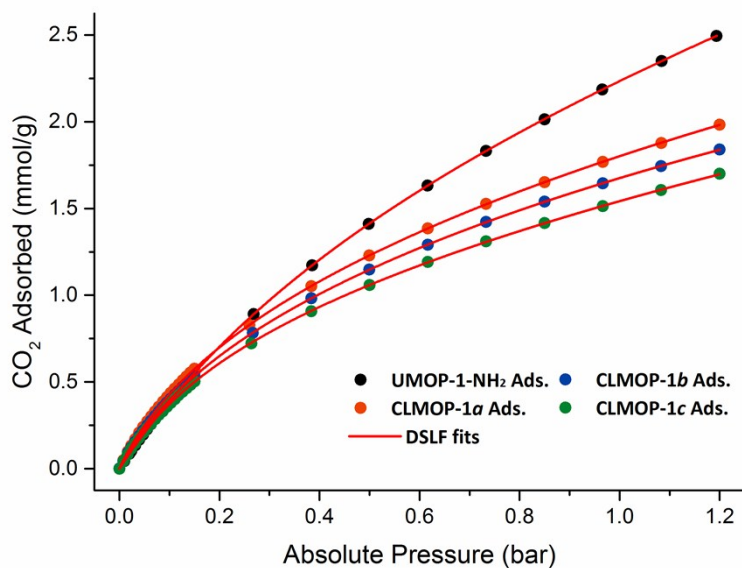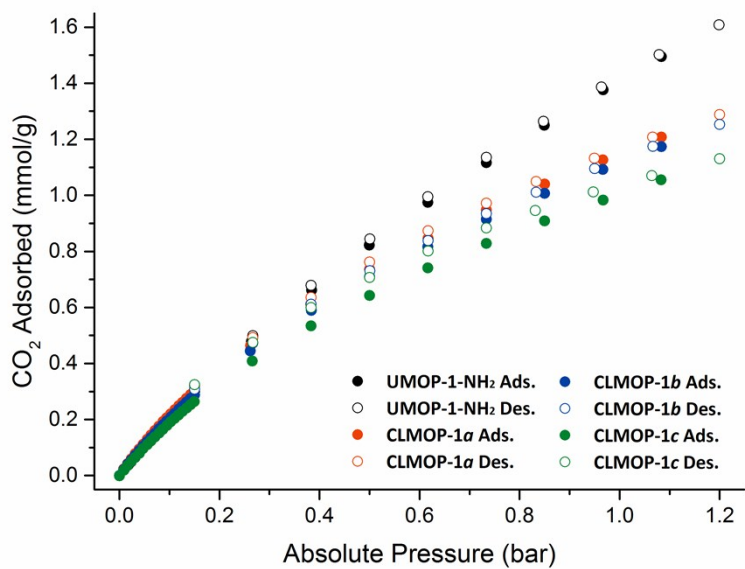
Figure S22. CO_2 isotherms (273K) of UMOP-1-NH$_2$ and CLMOPs fitted with DSLF equation.
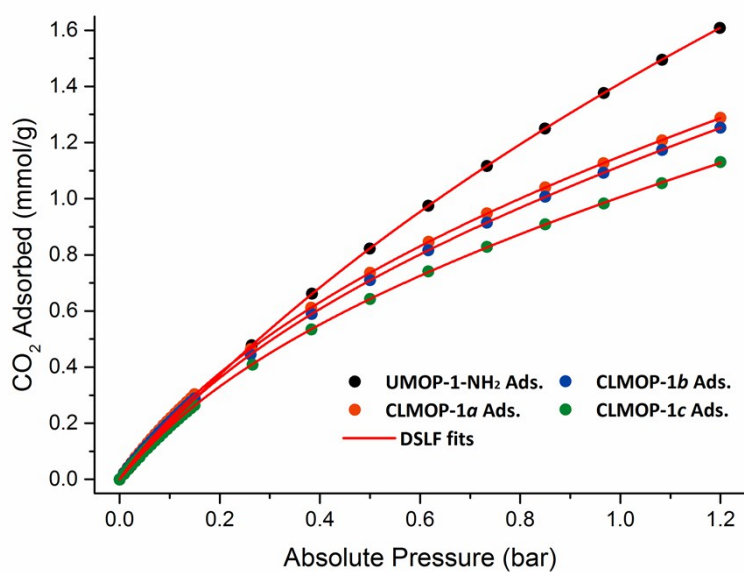
Table S4. Fitted parameters from DSLF fitting of CO_2 isotherms (273K) of UMOP-1-NH$_2$ and CLMOPs.

|	$q_{sat,A}$ (mmol/g)	b_A (bar^{-1})	α_A	$q_{sat,B}$ (mmol/g)	b_B (bar^{-1})	α_B	R^2
UMOP-1-NH$_2$	3.929	1.029	0.976	2.836	0.0927	2.018	0.999999
CLMOP-1a	0.981	3.547	0.936	5.726	0.221	0.938	0.999997
CLMOP-1b	0.841	3.759	0.950	4.528	0.287	0.935	0.999998
CLMOP-1c	7.996	0.150	0.805	0.587	5.494	1.068	0.999990

Figure S23. CO_2 isotherms (293K) of UMOP-1-NH_2 and CLMOPs.

**Figure S24.** CO_2 isotherms (293K) of UMOP-1-NH_2 and CLMOPs fitted with DSLF equation.

Table S5. Fitted parameters from DSLF fitting of CO_2 isotherms (293K) of UMOP-1-NH_2 and CLMOPs.

|	$q_{sat,A}$ (mmol/g)	b_A (bar^{-1})	α_A	$q_{sat,B}$ (mmol/g)	b_B (bar^{-1})	α_B	R^2
UMOP-1-NH_2	1.450	0.815	0.981	6.958	0.123	1.011	0.999999
CLMOP-1a	5.656	0.123	0.992	0.788	2.077	0.963	0.999997
CLMOP-1b	0.899	1.836	0.971	13.341	0.042	0.992	0.999999
CLMOP-1c	0.628	2.603	1.012	6.300	0.096	1.001	0.999984
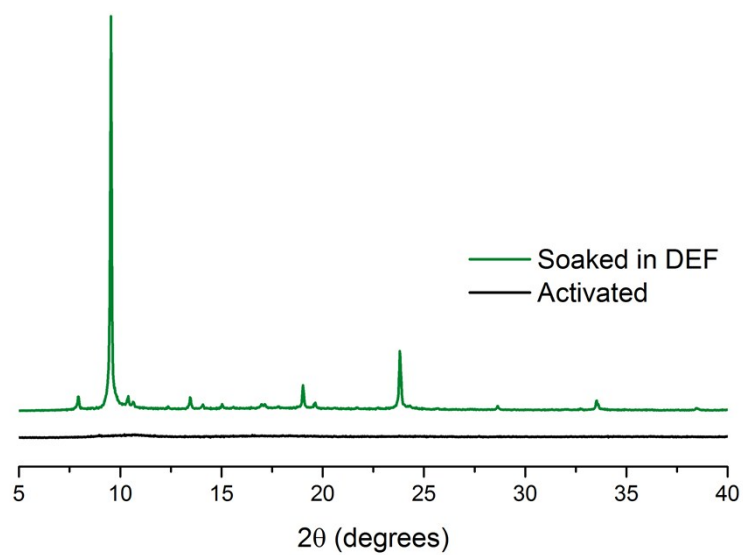
Figure S25. PXRD pattern of CLMOP-1*c* activated (black) and soaked in DEF (green). When CLMOP-1c (3 mg) was soaked in DEF (1 mL) for 20 min, its crystallinity was restored. This result suggests the tetrahedral cages are intact after activation.
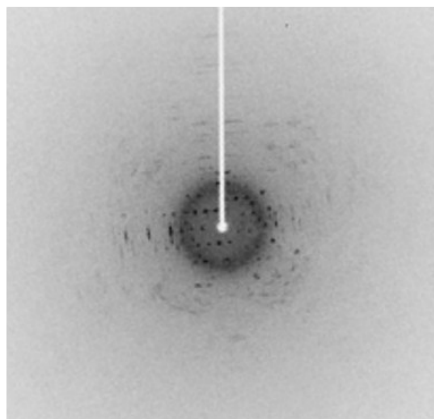
CLMOP-1*a*
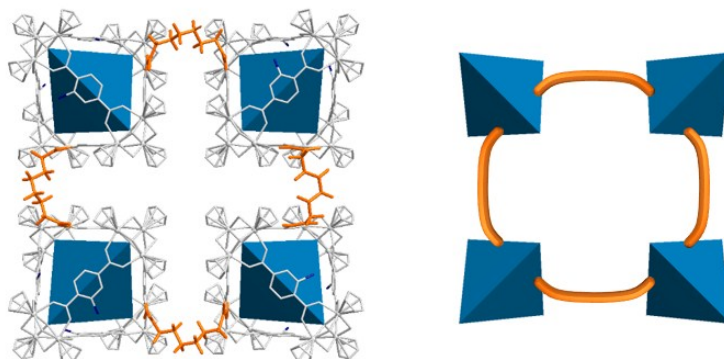
CLMOP-1*b*
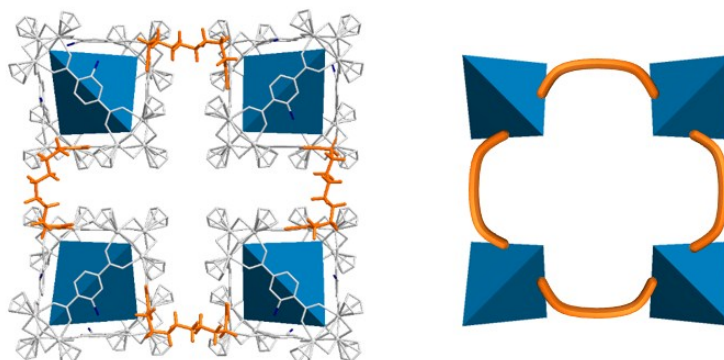
Figure S26. Structural models of CLMOP-1*a* and CLMOP-1*b*. In the models, the shortest unit (8.1 Å) was connected by L*a* and L*b*, respectively.

**Table S6.** Single crystal X-ray diffraction data of CLMOP-1*c*

	CLMOP-1*c*
Molecular formula[a]	$(Zr_{12}C_{141.6}H_{164}O_{47.4}N_6)Cl_6((C_2H_5)_2NH_2)_2$
Temperature	134K
Crystal system	Trigonal
Space group	*R*-3*m*
a (Å)	26.221(4)
c (Å)	60.059(12)
V (Å^3)	35760(12)
Z	6
ρ_{calc} (g·cm^{-3})	1.160
μ (mm^{-1})	2.715
R_1, $I > 2\sigma(I)$	0.0787
wR_2, $I > 2\sigma(I)$	0.2949

[a]Disordered solvent, cation, and amide with flexible moieties were treated with the SQUEEZE tool in PLATON[5]. The cation and flexible moieties were included in molecular formula. For the formula, ^{1}H-NMR data of CLMOP-1*c* was consulted.
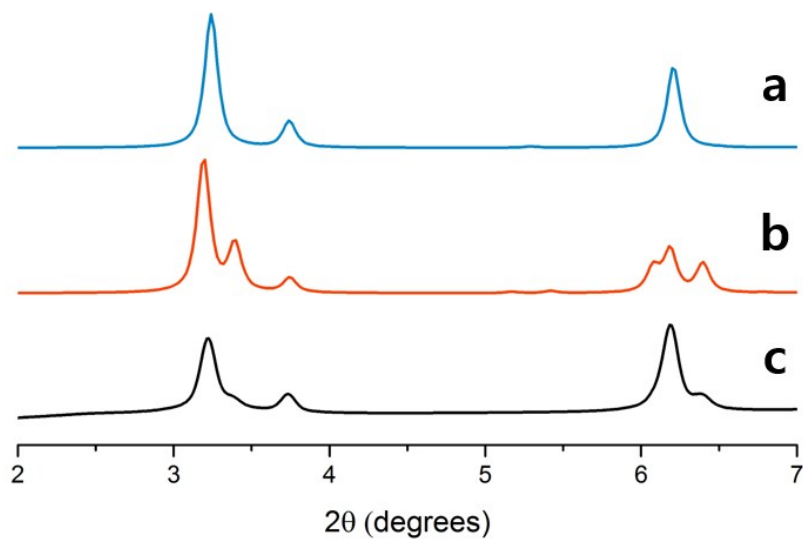
CLMOP-1*a*   **CLMOP-1*b***
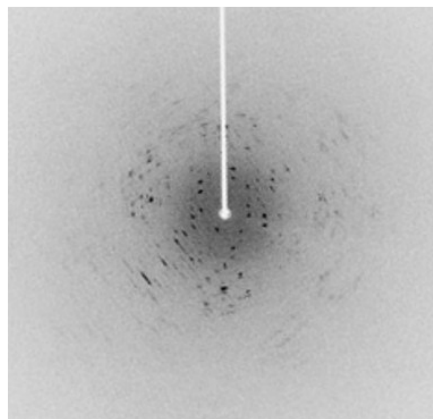
Figure S27. SCXRD spot images of CLMOP-1*a* and CLMOP-1*b*. Both images show poor single crystallinity.

Figure S28. (a) Simulated pattern from single crystal data of UMOP-1-NH$_2$, solved in *Fm-3m* space group. (b) Simulated pattern from single crystal data of CLMOP-1*c*, solved in *R*-3*m* space group. (c) Experimental PXRD pattern of CLMOP-1*c*

Reference

1. Hintz, H.; Wuttke, S. *Chem. Mater.* **2014**, *26*, 6722-6728.

2. Arvai, A. J.; Nielsen, C. *ADSC Quantum-210 ADX Program*, *Area Detector System Corporation*, Poway, CA, USA (1983).

3. Otwinowski, Z.; Minor, W. *Methods Enzymol*. **1997**, *276*, 307-326.

4. Sheldrick, G. M. *Acta Crystallogr. Sect. A* **2008**, *64*, 112-122.

5. Spek, A. L. *J. Appl. Crystallogr.* **2003**, *36*, 7-13.

6. Shin, J. W.; Eom, K.; Moon, D. *J. Synchrotron Rad.* **2016**, *23*, 369-373.

7. Hammersley, A. P.; Svensson, S. O.; Hanfland, M.; Fitch, A. N.; Hausermann, D. *High Pressure Research.* **1996**, *14*, 235-248.

8. McDonald, T. M.; Lee, W. R.; Mason, J. A.; Wiers, B. M.; Hong, C. S.; Long, J. R. *J. Am. Chem. Soc.* **2012**, *134*, 7056-7065.

9. Katz, M. J.; Brown, Z. J.; Colón, Y. J.; Siu, P. W.; Scheidt, K. A.; Snurr, R. Q.; Hupp, J. T.; Farha, O. K. *Chem. Commun.* **2013**, *49*, 9449-9451.